Calorimetric Investigations of Saturated Mixed-Chain Phosphatidylcholine Bilayer Dispersions†

Jeffrey T. Mason, Ching-hsien Huang,* and Rodney L. Biltonen

ABSTRACT: A series of saturated mixed-chain phosphatidylcholines were prepared whose *sn*-2 acyl chains are two, four, six, and eight carbon atoms shorter than the *sn*-1 acyl chain. The calorimetric behavior of multilamellar bilayers of these phosphatidylcholines in excess water is investigated. The phosphatidylcholines display cooperative phase transitions which are dependent upon both the difference in chain length and the position of the acyl chains on the glycerol backbone of the phospholipid. A model is proposed which suggests that the thermotropic behavior of the mixed-chain phosphatidylcholines results from progressively greater interdigitation of the acyl chains of the phospholipid across the bilayer center, in the gel state, as the chain-length difference is increased beyond a minimum value. The disruptive effect of the terminal methyl groups of the fatty acyl chains upon the bilayer packing stability is also stressed. Dispersions of some of the mixed-chain phosphatidylcholines display transition endotherms which appear to be composites of two or more individual transition peaks. The dependence of this behavior on the thermal history of the dispersions is investigated. It is proposed that these peaks arise from the ability of the phosphatidylcholines' acyl chains to pack in more than one interdigitated conformation in the gel state.

One of the most prominent features displayed by model membrane systems of synthetic phosphatidylcholines is the thermally induced gel ↔ liquid-crystalline phase transition. This property has been the subject of extensive experimental investigation [for a review, see Mabrey & Sturtevant (1978); Lee, 1975) as well as theoretical consideration (Jacobs et al., 1977). Although interesting in its own right, many recent investigations have shown that the gel ↔ liquid-crystalline phase transition may have important implications for the proper function of biological membranes (Nagle & Scott, 1978; Melchior & Stein, 1979; Boheim et al., 1980).

Until recently, studies of the thermal phase transition in model membrane systems have concentrated on synthetic phosphatidylcholines whose fatty acyl chains are saturated and of identical carbon number (Ladbrooke & Chapman, 1969; Mabrey & Sturtevant, 1976). Naturally occurring phosphatidylcholines, however, usually possess mixed fatty acids of varying chain length and degree of unsaturation with the 1-saturated-acyl–2-unsaturated-acyl chain configuration being the one most frequently encountered.

Attempts to investigate the thermal behavior of more biologically relevant phosphatidylcholines have recently been undertaken with the study of saturated mixed-chain phosphatidylcholines whose fatty acyl chains differ in carbon number (Keough & Davis, 1979; Stümpel et al., 1981; Chen & Sturtevant, 1981). Studies on bilayer dispersions of these phosphatidylcholines reveal that for acyl chain differences of two or four carbons, the thermal properties of the phosphatidylcholines are dependent upon both the difference in chain length and the position of the acyl chains on the phospholipid glycerol backbone. Thus, for example, it was found that for pairs of positional isomers, such as C(18):C(16)-PC,[1] C(16):C(18)-PC and C(18):C(14)-PC, C(14):C(18)-PC, the phosphatidylcholine with the longer chain in the 2-acyl position exhibits the higher T_m and ΔH of the pair. In addition, the T_m's of both members of the pair are found to lie between the T_m's of the corresponding like-chain phosphatidylcholines. The effects of the inequivalence of the two fatty acyl chains upon the bilayer hydrocarbon thickness (Keough & Davis, 1979) and the conformation of the terminal ends of the acyl chains (Stümpel et al., 1981) have been suggested as explanations for the observed pattern of thermotropic behavior in bilayers of these phosphatidylcholines.

In this investigation, we extend the previous studies by systematically varying the chain length of saturated mixed-chain phosphatidylcholines to include differences of two, four, six, and eight carbons. Differences in acyl chain number of six or more carbons are particularly interesting since binary mixtures of saturated like-chain phosphatidylcholines differing in acyl chain length by six carbon atoms are monotectic, showing lateral phase separation in the gel state (Mabrey & Sturtevent, 1976). The mixed-chain phosphatidylcholines present an interesting variation on the above studies since the acyl chains are forced to mix by virtue of being attached to the same glycerol backbone. We will show that the magnitude of the main thermal phase transition (ΔH, ΔS) in bilayers of these phosphatidylcholines can be rationalized by proposing that the phosphatidylcholine's fatty acyl chains progressively interdigitate across the bilayer center as the difference in acyl chain length is increased beyond a minimum value.

Dispersions of C(18):C(10)-PC and C(18):C(14)-PC were observed to display transition endotherms which appear to be a composite of two transition peaks. It is suggested that this

† From the Department of Biochemistry, University of Virginia School of Medicine, Charlottesville, Virginia 22908. *Received May 15, 1981.* This work was supported in part by Research Grant GM-17452 from the National Institute of General Medical Sciences, U.S. Public Health Service.

[1] Abbreviations used: C(18):C(18)-PC, 1,2-distearoyl-*sn*-glycero-3-phosphorylcholine; C(18):C(16)-PC, 1-stearoyl-2-palmitoyl-*sn*-glycero-3-phosphorylcholine; C(16):C(18)-PC, 1-palmitoyl-2-stearoyl-*sn*-glycero-3-phosphorylcholine; C(18):C(14)-PC, 1-stearoyl-2-myristoyl-*sn*-glycero-3-phosphorylcholine; C(14):C(18)-PC, 1-myristoyl-2-stearoyl-*sn*-glycero-3-phosphorylcholine; C(16):C(14)-PC, 1-palmitoyl-2-myristoyl-*sn*-glycero-3-phosphorylcholine; C(14):C(16)-PC, 1-myristoyl-2-palmitoyl-*sn*-glycero-3-phosphorylcholine; C(18):C(12)-PC, 1-stearoyl-2-lauroyl-*sn*-glycero-3-phosphorylcholine; C(18):C(10)-PC, 1-stearoyl-2-caproyl-*sn*-glycero-3-phosphorylcholine; C(10):C(18)-PC, 1-caproyl-2-stearoyl-*sn*-glycero-3-phosphorylcholine; TLC, thin-layer chromatography; GLC, gas–liquid chromatography; DSC, differential scanning calorimetry; NMR, nuclear magnetic resonance.

0006-2960/81/0420-6086$01.25/0

behavior most likely results from the ability of the interdigitated fatty acyl chains to adopt more than one packing configuration within the gel phase of the bilayer for these phosphatidylcholines.

Materials and Methods

Synthesis of Saturated Mixed-Chain Phosphatidylcholines. The method employed for the synthesis of the saturated mixed-chain phosphatidylcholines has been described in detail elsewhere (Mason et al., 1981) and will only be summarized here. Briefly, the starting substrate is a like-chain phosphatidylcholine whose fatty acyl chain is that desired to be in the 1-acyl position of the product mixed-chain phosphatidylcholine. These phosphatidylcholines were synthesized by rapidly stirring a mixture of *sn*-glycero-3-phosphorylcholine–$CdCl_2$ adduct, 4 equiv of the desired fatty acid anhydride, 1 equiv of 4-pyrrolidinopyridine, and glass beads in dry, ethanol-free chloroform at 35 °C. The resulting like-chain phosphatidylcholines were purified by elution from silicic acid employing a gradient of chloroform and methanol. The 2-acyl fatty acid of this substrate is removed by enzymatic hydrolysis with phospholipase A_2, and the resulting 1-acyl lysophosphatidylcholine is purified by crystallization from diethyl ether–methanol. The lysophosphatidylcholine is then reacylated with the anhydride of the fatty acid desired to be in the 2-acyl position of the mixed-chain product. The reacylation reaction is performed in dry, ethanol-free chloroform at 35 °C, employing the catalyst 4-pyrrolidinopyridine. The resulting mixed-chain phosphatidylcholine is then purified by elution from silicic acid, employing a gradient of chloroform and methanol. Finally, the phosphatidylcholine is recrystallized 3 times from acetone–chloroform (95:5), dried, and stored desiccated at −20 °C.

The fatty acid composition of the mixed-chain phosphatidylcholines was determined by transmethylation of the acyl chains of the phospholipid followed by analysis on GLC. The column conditions employed for the GLC analysis have been described elsewhere (Lippiello et al., 1979).

During the reacylation of the lysophosphatidylcholine, migration of the acyl chains can occur, resulting in contamination of the mixed-chain phosphatidylcholine by the positional isomer of the desired product. The amount of this contamination is determined by subjecting the mixed-chain product to enzymatic hydrolysis with phospholipase A_2 followed by recovery of the free fatty acids by TLC. The fatty acids were then methylated and analyzed by GLC. This result, and the overall fatty acid composition, yields the amount of positional isomer present in the mixed-chain product. The procedure employed for the synthesis of the mixed-chain phosphatidylcholines (Mason et al., 1981) has been designed to minimize acyl migration and yields products which are typically about 99 mol % isomerically pure.

Preparation of Samples for DSC. The mixed-chain phosphatidylcholine to be analyzed is lyophilized from benzene until constant weight. Then 10–15 mg of this lipid is dispersed in 1 mL of 50 mM KCl prepared from ultrapure KCl (J. T. Baker) and doubly glass-distilled, deionized water. This suspension is vortexed for 3–4 min at a temperature 5–10 °C above the phase transition of the phosphatidylcholine and then incubated at this temperature for an additional hour. A volume of ≈0.7 mL of freshly vortexed suspension is added to a stainless steel calorimeter cell with a hyperdermic syringe, and the cell is then tightly sealed. The sample cell is inserted into the calorimeter, which has been equilibrated at a temperature 10–15 °C below the expected phase transition temperature of the sample. The calorimeter run is started as soon as the sample cell has equilibrated with the calorimeter sink (typically 5–10 min).

Table I: Fatty Acid Analysis of the Mixed-Chain Phosphatidylcholines

phosphatidylcholine	M_r	F_1[a] (%)	F_2 (%)	isomeric impurity[b] (%)
1-stearoyl-2-stearoyl-PC	790			
1-stearoyl-2-palmitoyl-PC	762	50.4	49.6	1.0
1-stearoyl-2-myristoyl-PC	734	49.4	50.6	0.8
1-stearoyl-2-lauroyl-PC	706	50.8	49.2	0.8
1-stearoyl-2-caproyl-PC	678	49.7	50.3	0.7
1-caproyl-2-stearoyl-PC	678	49.2	50.8	1.1

[a] F_1 and F_2 are the percentage of the fatty acids designated to be at the 1-acyl and 2-acyl positions, respectively, of the mixed-chain PC relative to the total fatty acid present. This was established by transmethylation of the PC followed by GLC. The column conditions for the GLC have been described previously (Lippiello et al., 1979). [b] The amount (in mol %) of mixed-chain isomeric impurity present in the mixed-chain product. The 2-acyl fatty acid of the PC was hydrolyzed with phospholipase A_2, and the free fatty acids were recovered by TLC (Mason et al., 1981). The fatty acids were then transmethylated and analyzed by GLC. This result and the values of F_1 and F_2 allow for the calculation of the amount of isomeric impurity present in the product.

At the end of the calorimetric scan, the sample cell is removed from the calorimeter and the sample extracted. The cell is rinsed several times with chloroform–methanol (2:1), and the sample and washings are combined and dried under vacuum. The amount of phosphatidylcholine present is then determined by the method of inorganic phosphate (Gomori, 1942).

Some samples of C(18):C(14)-PC and C(18):C(10)-PC were subjected to special conditions of thermal history prior to being analyzed by DSC. These conditions will be described under Results as they arise.

Differential Scanning Calorimetry. The calorimetry was performed with a high-sensitivity DSC instrument of the heat conduction type based upon the design of Ross & Goldberg (1974). The construction and operation of this instrument has been described in detail elsewhere (Suurkuusk et al., 1976). Briefly, two matched stainless steel cells of about 1-mL capacity containing the sample and reference (water) are housed in aluminum blocks which are surrounded by a large, insulated copper heat sink. A thermopile between the two cells produces a differential voltage which is proportional to the temperature difference between the cells. This temperature difference can, in turn, be translated into the excess heat capacity of the solute phosphatidylcholine. During the calorimetric scan, the temperature of the heat sink is raised, and the temperature of the heat sink and differential cell voltage are recorded, as a function of time, on paper tape. All scans were performed at a scan rate of 0.26 K min^{-1} (15.7 °C h^{-1}) in the ascending temperature direction. At the end of the scan, the data recorded on the paper tape are fed into a computer and analyzed to produce an output of phosphatidylcholine excess heat capacity and enthalpy as a function of temperature. These data were used for the construction of the plots of excess heat capacity vs. temperature shown in the figures and the quantitative thermodynamic data given in Table II. Instrument base-line noise is better than ±25 μcal/deg, and absolute temperature determination is better than ±0.05 °C.

Results

Fatty Acid Analysis of the Mixed-Chain Phosphatidylcholines. Table I lists the fatty acid composition of the sat-

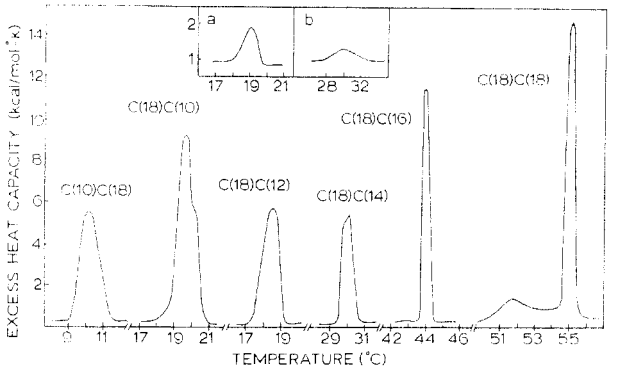

FIGURE 1: Endothermic phase transitions of multilamellar dispersions of C(10):C(18)-PC, C(18):C(10)-PC, C(18):C(12)-PC, C(18):C(14)-PC, C(18):C(16)-PC, and C(18):C(18)-PC are shown. The inset figures are (a) the pretransition of C(18):C(14)-PC and (b) the pretransition of C(18):C(16)-PC. The pretransition of C(18):C(18)-PC is shown to overlap the main thermal transition. Scans were performed for 10–15 mg/mL lipid in excess 50 mM KCl at a scan rate of 0.26 K min^{-1}. See Materials and Methods for details.

urated mixed-chain phosphatidylcholines synthesized for this study. As can be seen, these phosphatidylcholines average about 99 mol % purity with respect to the desired fatty acid composition and positional specificity. The mixed-chain phosphatidylcholines will thus yield an accurate estimate of the thermodynamics of the ideally pure corresponding phospholipids. This eliminates the necessity of estimating these parameters by the construction of phase diagrams for the positional isomers as has been done in past studies (Keough & Davis, 1979; Chen & Sturtevant, 1981).

Calorimetry of the Saturated Mixed-Chain Phosphatidylcholines. The endothermic transition profiles of the saturated mixed-chain phosphatidylcholine multilamellar bilayer dispersions in excess 0.05 M KCl are shown in Figure 1, and the corresponding thermodynamic parameters are listed in Table II. The mixed-chain phosphatidylcholines display cooperative phase transitions whose transition widths [with the acception of C(18):C(16)-PC] are considerably broader than those observed for saturated like-chain phosphatidylcholines. The transition temperatures of the phosphatidylcholines are observed, as expected, to increase with increasing molecular weight with the exception of C(18):C(10)-PC (T_m ~ 19.9 °C) and C(18):C(12)-PC (T_m = 18.5 °C). It is interesting to note that the transition enthalpy does not progressively increase as the length of the *sn*-2 fatty acyl chain approaches that of the *sn*-1 chain. Thus, the magnitude of the phase transition is not strictly determined by the length of the shorter of the two fatty acyl chains, as has been suggested by Stümpel (Stümpel et al., 1981).

The transition temperatures and enthalpies of the mixed-chain phosphatidylcholine bilayers are found to lie between the values for the corresponding like-chain phosphatidylcholines. The one exception is the value of ΔH for C(18):C(16)-PC which is below the value of ΔH observed for either C(16):C(16)-PC or C(18):C(18)-PC (Mabrey & Sturtevant, 1976). For the positional isomers C(18):C(10)-PC and C(10):C(18)-PC, the C(18):C(10)-PC, with the longer chain in the 1-acyl position, is seen to have the higher T_m and ΔH of the pair. This is opposite to the trends observed for other mixed-chain positional isomers that have been investigated (Keough & Davis, 1979; Stümpel et al., 1981; Chen & Sturtevant, 1981). An explanation for this behavior will be presented under Discussion.

The thermodynamic parameters reported here for C(18):C(18)-PC, C(18):C(16)-PC, and C(18):C(14)-PC agree well with previously published results (Mabrey & Sturtevant, 1976; Keough & Davis, 1979; Stümpel et al., 1981; Chen & Sturtevant, 1981). It should be noted that due to instrumental limitations in achieving a thermal steady state above 7 °C in our calorimeter, the C(10):C(18)-PC transition curve should not be considered to be of as high a resolution as those for the rest of the phosphatidylcholines. Thus, it is possible that additional fine structure that was not observed may exist in this endotherm.

Table II: Thermodynamic Parameters of the Mixed-Chain Phosphatidylcholines[a]

phosphatidylcholine	T_o (°C)	T_c (°C)	T_m (T_{m1}, T_{m2}) (°C)	$\Delta T_{1/2}$ (°C)	ΔH (kcal/mol)	ΔS (eu/mol)
C(10):C(18)-PC	9.1	11.5	10.1	1.21	7.9	27.9
C(18):C(10)-PC	18.2	20.9	19.7, 20.2	0.98	10.1	34.5
C(18):C(12)-PC	17.0	19.3	18.5	1.14	7.7	26.4
C(18):C(14)-PC	29.4	30.8	29.9, 30.1	0.73	5.6	18.5
c	17.9	19.7	19.1	1.03	1.3	4.5
C(18):C(16)-PC	43.7	44.6	44.1	0.46	7.2	22.7
d	27.6	32.4	30.1	2.65	0.7	2.3
C(18):C(18)-PC	54.3	55.8	55.1	0.51	10.3	31.4
C(18):C(18)-PC[b]	50.1	53.3	51.7	1.81	2.1	6.5
e	18.4	20.9	19.7, 20.2	1.09	10.4	36.2
f	18.9	20.5	19.8	0.94	9.7	33.1

[a] The thermodynamic parameters derived from the calorimetric scans of Figures 1 and 2. T_o and T_c are the onset and completion temperatures, respectively, of the thermal transitions. The transition temperature (T_m) is taken to be the temperature of the maximal excess heat capacity. For those transitions displaying two peaks, two transition temperatures (T_{m1}, T_{m2}) are reported. $\Delta T_{1/2}$ is the transition width at half-maximal excess heat capacity. ΔH is the transition enthalpy which is taken from the results of the computer analysis of the transition endotherm. ΔS is the transition entropy which is estimated from the Clausius equality as $\Delta S = \Delta H/T_m$, assuming a first-order equilibrium transition. For those transitions displaying two transition peaks, the values reported for $\Delta T_{1/2}$, ΔH, and ΔS are for the composite transition. Also, the average transition temperature, (T_{m1} + T_{m2})/2, is used in the calculation of ΔS. All scans were performed with 10–15 mg/mL of lipid in excess 0.05 M KCl and by employing a scan rate of 0.26 K min^{-1}. See the text for details. [b] Thermodynamic parameters of the C(18):C(18)-PC pretransition. [c] Pretransition (see Figure 1a). [d] Pretransition (see Figure 1b). [e] C(18):C(10)-PC transition (see Figure 2A). [f] C(18):C(10)-PC transition (see Figure 2B).

The C(18):C(16)-PC and C(18):C(14)-PC both display thermal pretransitions at a temperature below that of the main thermal transition. For the C(18):C(16)-PC (Figure 1b), both the T_m and ΔH of the pretransition are below those values observed for the pretransitions of the corresponding like-chain phosphatidylcholines. The C(18):C(14)-PC (Figure 1a) has a T_m between, but a larger ΔH than, the pretransitions of the corresponding like-chain phosphatidylcholines. The rest of the mixed-chain phosphatidylcholines did not display a pretransition above 7 °C.

The endothermic transition profiles of C(18):C(14)-PC and C(18):C(10)-PC both appear to be a composite of two transitions. In the case of C(18):C(14)-PC, the transition appears to consist of a large higher temperature peak (T_m taken as the maximum of the excess heat capacity) and a smaller low temperature peak that appears as a partially resolved shoulder (T_m taken as the point of inflection of the shoulder). A similar fine structure, but with greater resolution, was also observed in a high sensitivity DSC study of this mixed-chain phosphatidylcholine by Chen & Sturtevant (1981). For the C(18):C(10)-PC, the transition profile consists of a large lower temperature peak and a smaller higher temperature peak

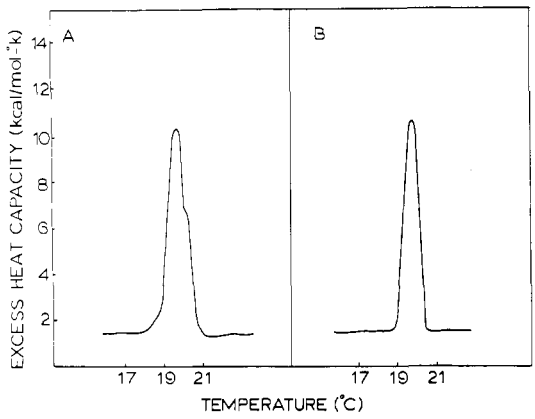

FIGURE 2: Effect of the rate of cooling of C(18):C(10)-PC bilayer dispersions on the endothermic transition profile. (A) Dispersions at 25 °C were rapidly frozen in dry ice–acetone (−80 °C), thawed, and immediately scanned from 10 °C. (B) Dispersions at 25 °C were slowly cooled through the phase transition at 1.5 °C h^{-1} and then scanned from 10 °C. Lipid concentrations were 10–15 mg/mL in excess 50 mM KCl, and a scan rate of 0.26 K min^{-1} was employed. See text for details.

which is observed as a partially resolved shoulder. The difference in temperature of these two peaks (0.5 °C) is larger than that observed in the C(18):C(14)-PC (0.2 °C). The dependence of these endotherms on the thermal history of the sample will be discussed below.

Thermal History of C(18):C(10)-PC and C(18):C(14)-PC Dispersions. The effect of the thermal history of C(18):C(10)-PC bilayer dispersions on the multiple peak transition endotherm was investigated. Figure 2 shows the effect of varying the rate at which the sample was cooled through the phase transition prior to the calorimetric scan. In Figure 2A, a sample of C(18):C(10)-PC dispersions at 25 °C was rapidly frozen (in about 5 s) in a dry ice acetone bath at −80 °C. The sample was then thawed, immediately added to the calorimeter, and scanned from 10 °C. The rapidly cooled sample displays the same two transition peaks that were observed for C(18):C(10)-PC in Figure 1. In Figure 2B, a sample of C(18):C(10)-PC dispersions at 25 °C was slowly cooled through the phase transition at 1.5 °C h^{-1} and then scanned from 10 °C. This endotherm, in contrast, displays only a single transition peak. This peak appears to correspond to the low temperature peak observed in the rapidly cooled sample (Table II). Thus, it appears that the high temperature peak represents a metastable bilayer packing phase which either disappears or becomes unresolvable when the sample is slowly cooled through the phase transition.

Samples of C(18):C(14)-PC dispersions were cooled either rapidly or slowly through the phase transition in analogy to the experiments described in Figure 2 for C(18):C(10)-PC. In this case, however, the C(18):C(14)-PC transition profile appears to be independent of these manipulations (data not shown) and always yields a transition profile identical with that shown in Figure 1 for C(18):C(14)-PC.

Discussion

The thermal phase transition behavior of these mixed-chain phosphatidylcholines can be rationalized by taking into account the effect of the chain-length inequivalence upon the hydrocarbon packing arrangements within the interior of phospholipid bilayer. X-ray diffraction studies on single crystals of dimyristoyl-L-α-phosphatidylcholine dihydrate (Pearson & Pascher, 1979) have revealed that in like-chain phosphatidylcholines the two acyl chains are conformationally inequivalent. The initial segment of the *sn*-2 acyl chain extends

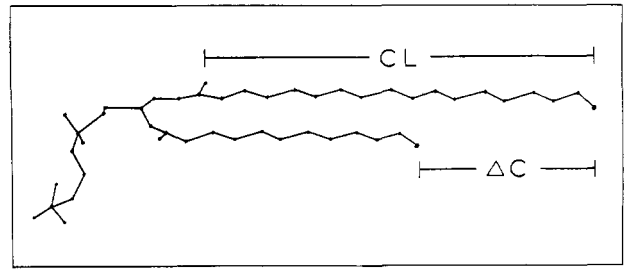

FIGURE 3: Molecular diagram of 1-stearoyl-2-lauroyl-*sn*-glycero-3-phosphorylcholine demonstrating the parameters used in the calculation of the chain parameter ($\Delta C/CL$). $\Delta C = |n_1 - n_2 + 1.5|$ where n_1 and n_2 are the number of carbons in the *sn*-1 and *sn*-2 acyl chains, respectively. CL is the length (in carbon bonds) of the longer of the two fatty acyl chains; thus, the larger of the two values $n_1 - 1$ or $n_2 - 2.5$ is employed. See text for details.

perpendicular to the *sn*-1 chain but then bends abruptly at the C(2) atom so that the remainder of the *sn*-2 chain runs parallel to the linear *sn*-1 fatty acyl chain in the single crystal. Because of this abrupt bend, the terminal methyl groups of the two alkyl chains are not in register but are displaced in length by a distance of ~3.7 Å. In the gel phase of the bilayer, ^2H NMR and neutron diffraction studies of saturated like-chain phosphatidylcholines indicate that this conformational inequivalence persists but that the displacement in length is reduced to about 1.8 Å (1.5 C–C bond lengths) (Büldt et al., 1978; Zacci et al., 1979).

In a previous communication (Mason & Huang, 1981), we suggested that for like-chain phosphatidylcholines in the gel phase, this conformational inequivalence requires the methyl terminus of the *sn*-1 acyl chain to be distorted, possibly by trans ↔ gauche isomerization, to fill the space under the *sn*-2 acyl chain in order not to leave a region void of van der Waals contacts. This terminal distortion is further suggested to perturb the conformational statistics of the rest of the hydrocarbon chains as well as the interaction between chains in the bilayer. Consequently, it was shown that the methyl terminal distortion can affect the magnitude of the thermal phase transition in bilayers of these like-chain phosphatidylcholines. Indeed, the transition entropy and temperature were shown to decrease linearly with an increase in methyl terminal perturbation (P) which can be quantitatively defined as the distorted methyl terminal region (1.5 C–C bonds) relative to the chain length of the saturated like-chain phosphatidylcholines (Mason & Huang, 1981).

It has been shown by Seelig & Seelig (1980) that an abrupt bend of the initial segment of the *sn*-2 chain persists for the mixed 1-saturated–2-unsaturated phosphatidylcholines in bilayers, and the conformational inequivalence of the two chains is independent of the exact composition of the fatty acyl chains. For the mixed-chain saturated phosphatidylcholines considered here, it is thus reasonable to assume that this conformational inequivalence, due to the bent nature of the initial *sn*-2 segment, is conserved despite the actual difference in carbon number of the two chains.

In Figure 3, we define the two parameters that were employed to characterize the chain-length inequivalence of the mixed-chain phosphatidylcholines. The parameter ΔC is the absolute difference in chain length of the two fatty acyl chains and is given by the equation $\Delta C = |n_1 - n_2 + 1.5|$, where n_1 and n_2 are the number of carbons in the *sn*-1 and *sn*-2 acyl chains, respectively. CL is the length of the longer of the two fatty acyl chains (in carbon bonds) of the mixed-chain phosphatidylcholine; thus, for each phosphatidylcholine, the larger of the two values $n_1 - 1$ or $n_2 - 2.5$ is employed. The magnitude of the chain inequivalence relative to the overall

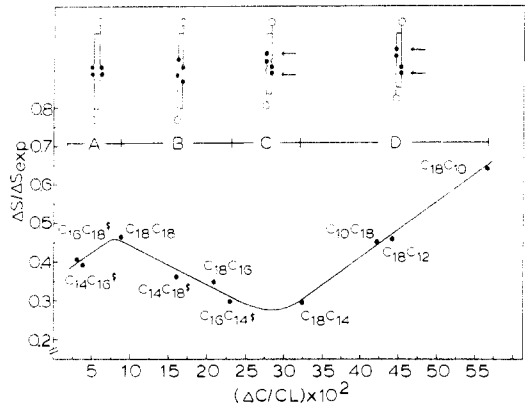

FIGURE 4: Plot of the magnitude of the thermal phase transition as a function of the chain parameter for the saturated mixed-chain phosphatidylcholines. The trends displayed by the plot have been divided into four regions (A–D), and the acyl chain packing suggested to exist within these regions are diagramatically represented above each region. The size of the acyl chain terminal methyl groups has been exaggerated in order to emphasize thier perturbing effect upon the acyl chain packing. Values of the phosphatidylcholines marked with the symbol \$ have been calculated from the data of Chen & Sturtevant (1981). See text for details.

chain length is then given by $\Delta C/CL$. In Figure 4, we have plotted the chain parameter, $\Delta C/CL$, against the magnitude of the main thermal phase transition, taken as the transition entropy $\Delta S/\Delta S_{exp}$. Here, the transition entropy has been divided by a normalizing factor ΔS_{exp} (the expected transition entropy). Since the main transition of phospholipids in bilayers has been attributed primarily to the hydrocarbon melting transition (Nagle & Wilkinson, 1978), a reasonable estimate for the maximal transition entropy expected for a given phosphatidylcholine would be the fusion entropy for the corresponding free bulk fatty acids (Mason & Huang, 1981). This entropy is given by the relationship $\Delta S_{exp} = 1.9$ eu/mol $\times (n_1 + n_2)$ on the basis of the fusion entropy per carbon unit reported for bulk fatty acids (Phillips et al., 1969; Schaerer et al., 1955).

As shown in Figure 4, the trends displayed by the saturated mixed-chain phosphatidylcholines can be divided into four regions (regions A–D, Figure 4). The packing associations of the mixed-chain phospholipids in bilayers suggested to exist within these four regions are diagramatically represented in Figure 4 above each of the regions. The values for the phosphatidylcholines marked with the symbol \$ have been calculated from the data of Chen & Sturtevant (1981).

Region A. The value of ΔC for C(16):C(18)-PC and C(14):C(16)-PC is 0.5, meaning that the terminal methyl groups of the two acyl chains are separated by only a distance of about one-half carbon–carbon bond length in these phosphatidylcholines. Since the terminal methyl groups occupy about twice the effective volume of a methylene carbon unit (Reiss-Husson & Luzzati, 1964; Flory, 1969), the close proximity of the terminal methyls can be expected to greatly distort the chain packing in the center of the bilayer. Thus, as is shown in the schematic figure for region A, this distortion is accommodated by an increase in the effective volume per CH_2 near the methyl terminus of the acyl chains.

For C(18):C(18)-PC, the value of ΔC is 1.5 C–C bond lengths, meaning that the terminal methyl groups will be packed next to a methylene carbon rather than another methyl group. This is an energetically more favorable situation and explains the increase in the magnitude of the phase transition with increasing $\Delta C/CL$ within region A.

Region B. The magnitude of the thermal phase transition for the four phosphatidylcholines in region B decreases in linear correlation to an increase in $\Delta C/CL$ (linear correlation coefficient = 0.943). We feel that this is a strong linear correlation, considering that two of the values are taken from this work and two are literature values (Chen & Sturtevant, 1981). We propose that the phosphatidylcholines in this region adopt packing associations analogous to those of saturated like-chain phosphatidylcholines without interdigitation of the acyl chains across the bilayer center. As discussed above, the displaced methyl terminus of the acyl chains will introduce disorder into the bilayer gel phase packing. This, in turn, will cause a decrease in the magnitude of the phase transition as the distortion due to the inequivalence of the acyl chains increases relative to the overall chain length. This same linear relationship has been demonstrated for saturated like-chain phosphatidylcholines (Mason & Huang, 1981) where ΔC remains constant at 1.5 C–C bonds while the chain length is varied.

Region C. In region C, the linear trend observed to exist within region B stops as $\Delta S/\Delta S_{exp}$ reaches an apparent minimum value, after which the magnitude of the phase transition starts to increase as $\Delta C/CL$ increases. This pattern can be interpreted in the following manner. Once the distortion introduced into the bilayer by the chain-length inequivalence has reached a maximum value, the packing associations suggested to exist within region B are no longer stable. Thus, this packing association gives way to a new packing arrangement of the acyl chains as the bilayer attempts to compensate for the disruptive effect of the chain-length inequivalence.

Although there are a number of possible mechanisms whereby the bilayer could compensate for the chain inequivalence (such as tilting of the phospholipid acyl chains), the simplest explanation would seem to be for the acyl chains to adopt a bilayer interleaflet packing configuration. Thus, we propose that in the gel phase of the bilayer the phosphatidylcholines' acyl chains will interdigitate across the bilayer center, allowing the diplaced terminal ends of the acyl chains to pack in such a way that the short chain of one lipid in one leaflet will pack, end to end, with the long chain of another lipid in the opposing leaflet of the bilayer. This packing arrangement will compensate for the chain inequivalence and also increase the stability of the bilayer state. This interdigitated packing arrangement is shown in the schematic diagrams of lipid molecules for regions C and D in Figure 4. The area between the arrows in these figures is the region of interleaflet overlap of the terminal ends of the acyl chains.

Region D. We propose that within region D the mixed-chain phosphatidylcholines pack in a fully interdigitated arrangement in the bilayer gel phase and that the relative depth of interdigitation increases as the value of the chain parameter, $\Delta C/CL$, increases. It can be seen that the magnitude of the phase transition increases in strong linear correlation to an increase in $\Delta C/CL$ (linear correlation coefficient = 0.997) within region D. This suggests that the interdigitated packing arrangement must be the dominant, if not exclusive, packing arrangement within this region. An interdigitated packing arrangement has also been suggested as an explanation for the thermotropic behavior of synthetic sphingomyelins (Barenholz et al., 1976). The difference in chain length between the sphingosine chain and the acyl chain in the sphingomyelins may produce bilayer packing requirements analogous to the saturated mixed-chain phosphatidylcholines considered here. It is interesting to note, in this context, that X-ray studies (Tardieu et al., 1973) have revealed a fully interdigitated acyl chain conformation for C(18):C(10)-PC in the crystalline C phase. This conclusion was based upon the observation that

the unit cell dimensions of C(18):C(10)-PC in the crystalline phase are identical with the unit cell dimensions of 1,2-dimyristoyl-*sn*-glycero-3-phosphorylcholine.

The reason for the increase in the magnitude of the phase transition with an increase in the depth of interdigitation can be rationalized by, again, considering the disordering effects of the terminal methyl groups on the hydrocarbon chain packing. To understand this interpretation, one needs to consider the effect of nitroxide electron spin-labels upon bilayer dynamics. It has been shown that when the nitroxide spin-label is attached to the acyl chains of saturated like-chain phosphatidylcholines in multilamellar bilayers (Hubbell & McConnell, 1971), the spin-label bilayer order parameter increases linearly as the label is moved from the methyl end of the chain toward the carbonyl carbon. It has been suggested (Seelig & Seelig, 1974) that the spin-label is large enough to disrupt the packing of the hydrocarbon chains in its vicinity. However, when the spin label is moved near the glycerol backbone, the order parameter (S_{mol}) measured by the spin-label becomes very close to the corresponding value, as measured by ^{2}H NMR employing the non perturbing deuterium isotope as a probe (Seelig & Seelig, 1974). It is also evident that the perturbation of the ^{19}F-labeled acyl chain phospholipids, as judged by calorimetry (Sturtevant et al., 1979) and ^{2}H NMR (Oldfield et al., 1980), becomes quite small as the ^{19}F label is moved near the glycerol backbone. These facts strongly suggest that the packing properties of the methylene segments near the glycerol backbone are less likely to be severely affected by structurally perturbing probes than the rest of the fatty acyl chain.

The point of location of the terminal methyl groups in the interdigitated bilayer (as indicated by the arrows in Figure 4) can be envisioned to behave much like the nitroxide spin-label in disrupting the acyl chain packing in their vicinity. Increasing the depth of interdigitation will serve to move the location of the methyl terminus more toward the bilayer interface region where the relatively bulky methyl groups will exert a less disruptive effect upon the overall lateral packing of hydrocarbon chains in the multilamellar bilayer. These observations can account for the increase in the magnitude of the phase transition within region D as $\Delta C/CL$, and thus the relative depth of interdigitation, increases.

We would now like to address the nature of the multiple peak transition endotherms observed for dispersions of C(18):C(10)-PC and C(18):C(14)-PC. The multiple peak behavior of the C(18):C(10)-PC dispersions can be related to the thermal history of the sample in a simple way. It would appear that there are two different packing phases present in the gel state of this phosphatidylcholine. One phase is thermodynamically stable (lower temperature peak), and the other (high temperature peak) is a metastable phase, a "kinetic trap" rather than an equilibrium gel state. As revealed in Figure 2B, when the dispersion is cooled through the phase transition slowly (1.5 °C h^{-1}), the metastable phase can overcome the activation energy barrier and anneal to the stable packing phase; hence, only the lower peak is observed. When the dispersion is cooled through the transition rapidly (rapid freezing or 10 °C h^{-1}), however, the bilayer will enter the gel phase before all of the metastable phase can anneal, and a kinetically trapped phase, as manifested by a higher temperature peak, will be observed (Figure 2A).

The small difference in energy of about $^1/_2kT$ and an apparent low activation energy of conversion of the metastable to stable packing phase would suggest that these phases differ only subtly in packing configuration. It is tempting to suggest that the two transition peaks arise from coexisting regions of interdigitated and noninterdigitated phosphatidylcholines within the bilayer gel phase. Region B of Figure 4 is postulated to represent the noninterdigitated packing arrangement for the mixed-chain phosphatidylcholines. The linear relationship within this region can be seen to extrapolate to $\Delta S/\Delta S_{exp} = 0$ when $\Delta C/CL = 0.46$. However, $\Delta C/CL = 0.56$ for C(18):C(10)-PC, suggesting that a noninterdigitated packing conformation cannot exist for this phosphatidylcholine. Even if such a noninterdigitated phase did exist, it would be expected to be highly disordered and have a phase transition temperature well below that of the more stable interdigitated packing phase.

The most reasonable interpretation is to suggest that these peaks arise from the ability of the interdigitated chains to pack in more than one conformation within the bilayer gel phase of this phosphatidylcholine. As the bilayer is lowered through the phase transition, rotomerically disordered regions of the acyl chains can become trapped in metastable packing arrangements as the phosphatidylcholines' acyl chains interdigitate. If the cooling rate is slow, the metastable phases will be able to anneal to the thermodynamically most stable interdigitated packing phase with a minimum number of gauche isomers. A rapid cooling rate, however, can kinetically trap these metastable states and give rise to the observed two peak endotherm.

The multiple peak behavior of C(18):C(14)-PC dispersions does not appear to be related, in any simple way, to the thermal history of the sample. From Figure 4 it can be seen that C(18):C(14)-PC lies within region C where interdigitation of the phosphatidylcholine acyl chains in the bilayer gel state is proposed to be just beginning to occur. The close proximity of the terminal methyl groups in the interdigitated phase can, as discussed above, be expected to disorder the interdigitated region. Also, the value of $\Delta C/CL$ for C(18):C(14)-PC is 0.32, which indicates that noninterdigitated regions of C(18):C(14)-PC could possibly be stable and exist within the bilayer gel phase. The possible existence of coexisting regions of interdigitated and noninterdigitated acyl chains within C(18):C(14)-PC bilayers has also been suggested by Chen & Sturtevant (1981). These observations suggest that the bilayer center of C(18):C(14)-PC dispersions may be in a relatively dynamic state even in the gel phase of the bilayer. Thus, interconverting phases of interdigitated acyl chains and possibly coexisting regions of interdigitated and noninterdigitated phosphatidylcholines may exist within the bilayer. This would account for the insensitivity of the transition endotherm to the exact thermal history of the sample.

Finally, a multiple peak transition endotherm has been observed for C(16):C(14)-PC (Chen & Sturtevant, 1981). Although no resolvable fine structure was observed for dispersions of C(18):C(12)-PC and C(10):C(18)-PC in our study, these transitions are very broad, and the possibility exists that a multiple peak transition for these phosphatidylcholines might be revealed at higher resolution. Thus, a multiple peak transition endotherm could possibly be a general characteristic of mixed-chain phosphatidylcholines possessing interdigitated acyl chains in the bilayer gel phase. Further work is clearly necessary to clarify this idea. We are attempting to employ X-ray diffraction studies in order to better clarify these points.

Acknowledgments

We thank Anthony V. Broccoli for expert technical assistance. We also wish to acknowledge Dr. Forrest Anthony for assistance in the operation of the differential scanning calo-

rimeter and Marilyn Jackson for critical reading of the manuscript.

References

Barenholz, Y., Suurkuusk, J., Mountcastle, D., Thompson, T. E., & Biltonen, R. L. (1976) *Biochemistry 15*, 2441.
Boheim, G., Hanke, W., & Eibl, H. (1980) *Proc. Natl. Acad. Sci. U.S.A. 77*, 3403.
Büldt, G., Gally, H. U., Seelig, A., Seelig, J., & Zaccai, G. (1978) *Nature (London) 271*, 182.
Chen, S. C., & Sturtevant, J. M. (1981) *Biochemistry 20*, 713.
Flory, P. J. (1969) *Statistical Mechanics of Chain Molecules*, Wiley-Interscience, New York.
Gomori, G. (1942) *J. Lab. Clin. Med. 27*, 955.
Hubbell, W. L., & McConnell, H. M. (1971) *J. Am. Chem. Soc. 93*, 314.
Jacobs, R. E., Hudson, B. S., & Anderson, H. C. (1977) *Biochemistry 16*, 4349.
Keough, K. M. W., & Davis, P. J. (1979) *Biochemistry 18*, 1453.
Ladbrooke, B. D., & Chapman, D. (1969) *Chem. Phys. Lipids 3*, 304.
Lee, A. G. (1975) *Prog. Biophys. Mol. Biol. 29*, 3.
Lippiello, P. H., Holloway, C. T., Garfield, S. A., & Holloway, P. W. (1979) *J. Biol. Chem. 254*, 2004.
Mabrey, S., & Sturtevant, J. M. (1976) *Proc. Natl. Acad. Sci. U.S.A. 73*, 3862.
Mabrey, S., & Sturtevant, J. M. (1978) *Methods Membr. Biol. 9*, 237.
Mason, J. T., & Huang, C. (1981) *Lipids 16*, 604.
Mason, J. T., Broccoli, A. V., & Huang, C. (1981) *Anal. Biochem. 113*, 96.
Melchior, D. L., & Stein, J. M. (1979) *Prog. Surf. Membr. Sci. 13*, 211.
Nagle, J. F., & Scott, H. L. (1978) *Phys. Today 31*, 38.
Nagle, J. F., & Wilkinson, D. A. (1978) *Biophys. J. 23*, 159.
Oldfield, E., Lee, R. W. K., Meadows, M., Dowd, S. R., & Ho, C. (1980) *J. Biol. Chem. 255*, 11652.
Pearson, R. H., & Pascher, I. (1979) *Nature (London) 281*, 499.
Phillips, M. C., Williams, R. M., & Chapman, D. (1969) *Chem. Phys. Lipids 3*, 234.
Reiss-Husson, F., & Luzzati, V. (1964) *J. Phys. Chem. 68*, 3504.
Ross, P. D., & Goldberg, R. N. (1974) *Thermochim. Acta 10*, 143.
Schaerer, A. A., Busso, C. J., Smith, A. E., & Skinner, L. B. (1955) *J. Am. Chem. Soc. 77*, 2017.
Seelig, A., & Seelig, J. (1974) *Biochemistry 13*, 4839.
Seelig, J., & Seelig, A. (1980) *Q. Rev. Biophys. 13*, 19.
Stümpel, J., Nicksch, A., & Eibl, H. (1981) *Biochemistry 20*, 662.
Sturtevant, J. M., Ho, C., & Reimann, A. (1979) *Proc. Natl. Acad. Sci. U.S.A. 76*, 2239.
Suurkuusk, J., Lentz, B. R., Barenholz, Y., Biltonen, R. L., & Thompson, T. E. (1976) *Biochemistry 15*, 1393.
Tardieu, A., Luzzati, V., & Reman, F. C. (1973) *J. Mol. Biol. 75*, 711.
Zacci, G., Büldt, G., Seelig, A., & Seelig, J. (1979) *J. Mol. Biol. 134*, 693.

Specificity of the Bacteriophage PBS2 Induced Inhibitor of Uracil-DNA Glycosylase†

Peter Karran, Richard Cone,‡ and Errol C. Friedberg*

ABSTRACT: The purified PBS2 phage-coded inhibitor of uracil-DNA glycosylase (Ura-DNA glycosylase) from *Bacillus subtilis* has been tested for its ability to inhibit this enzyme isolated from other prokaryotic and from eukaryotic sources. In addition, the inhibitor has been assayed for its effect on DNA glycosylases specific for other base residues in DNA. The data indicate that Ura-DNA glycosylases from a variety of sources are equally sensitive to inhibition by the inhibitor. DNA glycosylases specific for base residues in DNA other than uracil are not inhibited by the PBS2-coded inhibitor.

The DNA glycosylases comprise a group of enzymes that initiate repair of DNA by cleavage of the glycosyl bond of damaged or inappropriate bases in DNA. To date, several distinct DNA glycosylases, each with an apparently stringent substrate specificity, have been isolated from both prokaryotic and eukaryotic organisms [for recent reviews, see Lindahl (1979) and Duncan (1981)]. These include separate glycosylases acting on DNA containing uracil (Lindahl et al., 1977; Cone et al., 1977; Talpaert-Borle et al., 1979; Caradonna & Cheng, 1980; Cone & Friedberg, 1981), hypoxanthine (Karran & Lindahl, 1978; Karran, 1981), 3-methyladenine (Laval, 1977; Riazuddin & Lindahl, 1978), 7-methylguanine residues containing a cleaved imidazole ring [2,6-diamino-4-hydroxy-5-(*N*-methylformamido)pyrimidine (FaPy)[1] (Chetsanga & Lindahl, 1979), urea (Breimer & Lindahl, 1981), ring-saturated thymine monoadducts (Demple & Linn, 1980), pyrimidine dimers (Haseltine et al., 1980; Radany & Friedberg, 1980; Seawell et al., 1980), and intact 7-methylguanine (Cathcart & Goldthwait, 1981; Laval et al., 1981; Margison

† From the MRC Cell Mutation Unit, Unversity of Sussex, Sussex BN1 9QG, England (P.K.), and the Laboratory of Experimental Oncology, Department of Pathology, Stanford University, Stanford, California 94305 (R.C. and E.C.F.). *Received April 21, 1981.* Studies from Stanford University were supported by Research Grant CA 12428 from the U.S. Public Health Service and by Contract DE-AS03-76SF70032 with the U.S. Department of Energy.

‡ Present address: School of Medicine, University of Cincinnati, Cincinnati, OH.

[1] Abbreviations used: Ura-DNA glycosylase, uracil-DNA glycosylase; FaPy, 2,6-diamino-4-hydroxy-5-(*N*-methylformamido)pyrimidine; Hyp-DNA glycosylase, hypoxanthine-DNA glycosylase (Hx in figures); AP, apurinic/apyrimidinic; Hepes, *N*-(2-hydroxyethyl)piperazine-*N*′-ethanesulfonic acid; EDTA, ethylenediaminetetraacetic acid.

0006-2960/81/0420-6092$01.25/0